land

MDPI

Article

Vegetation drastically reduces wind erosion: An implementation of the RWEQ in the Mongolian Gobi Steppe

Isita Talukdar [1,*], Virginia Anne Kowal[2], Binbin Huang [3], and Charlotte Weil [4]

[1] 5269 Manderston Drive, San Jose, CA 95138, USA;
[2] Natural Capital Project, Woods Institute for the Environment, Stanford University, 327 Campus Drive; Bass Biology Building 123; Stanford, CA 94305; ginger.kowal@gmail.com ; Phone: 828-775-2996
[3] State Key Laboratory of Urban and Regional Ecology, Research Center for Eco-Environmental Sciences, Chinese Academy of Sciences, 18 Shuangqing Road, Haidian District, Beijing, 100085, China; 17190196351@163.com ; Phone: +8617190196351
[4] EPFL ENAC-IT; GC D1 398; Station 18; CH-1015 Lausanne; charlotte.weil@epfl.ch ; Phone: +41 21 693 92 12
* Correspondence: isitatalukdar@gmail.com ; Phone: 669-400-6142

Abstract: Soil loss prevention is an important ecosystem service for protecting human and environmental health. Using spatio-temporal climate and environmental data of the Eastern Gobi Steppe, a region missing from previous studies of Mongolian wind erosion, we implement the Revised Wind erosion EQuation (RWEQ) model to estimate soil loss. A replicable pipeline is developed to perform these computations, and made available openly. Soil loss is estimated on a monthly basis to analyze seasonal variations. The results show that the annual total soil loss is 61 * 10^{10} kg over an area of 69.3 * 10^{3} km^2, which is about 9000 tonnes (the weight of 1492 African elephants) over an area equivalent to this of Ireland. Increasing fractional vegetation coverage to a uniform 50% coverage (doubling current vegetation coverage in every 1 km^2) could reduce soil loss by 60%, highlighting the importance of protecting and increasing vegetation coverage in ecosystem service preservation.

Keywords: wind erosion, soil loss, ecosystem services, revised wind erosion equation, Gobi Steppe

Citation: Lastname, F.; Lastname, F.; Lastname, F. Title. *Land* **2022**, *11*, x. https://doi.org/10.3390/xxxxx

Academic Editor: Firstname Lastname

Received: date
Accepted: date
Published: date

Publisher's Note: MDPI stays neutral with regard to jurisdictional claims in published maps and institutional affiliations.

Copyright: © 2022 by the authors. Submitted for possible open access publication under the terms and conditions of the Creative Commons Attribution (CC BY) license (https://creativecommons.org/licenses/by/4.0/).

0. SOFTWARE AVAILABILITY

The Python code of the model implemented in this paper is available in: https://github.com/charlottegiseleweil/winderosion. The README file includes a usage example, as well as a link to a sample data set.

1. Introduction

Soil loss due to wind erosion is a grave problem for semiarid and arid areas, where the lack of precipitation and scant vegetation coverage cannot prevent surface materials from being blown away by strong and frequent winds (Zhibao, 2000). This can lead to desertification, to severe soil coarseness, infertility, and dryness, which affect the ability to grow crops for sustenance (Duniway, 2019; Zhao, 2006). Wind erosion also creates sandstorms, and air pollution which affect pulmonary health (Li, 2005). A study done in Phoenix, Arizona, USA, found ~~that~~ "that the cropland wind erosion was responsible for 55% and 51% of total PM_{10} over Phoenix", with PM_{10} meaning dust particulate matter with diameter 10 μm and smaller including that caused by wind erosion (Joshi, 2021). Another study in Slovakia concluded that soil particles from up to a depth of 5 cm were displaced by wind, with the soil surface becoming "much rougher" (Lackóová, 2021). Indeed, the soil particles that enter the air from sandstorms are easily inhalable and can cause significant respiratory ailments due to oxidative stress, as they are embedded into deep lung tissue and the subepithelial environment (Saxton, 2001; Griffin, 2007). Such dust particulates can also increase the rates of anemia, liver and kidney disease, and asthma (Dou,

2022). For all these reasons, soil erosion control is one of the fundamental ecosystem services for human welfare (Fu, 2011).

Wind erosion is caused by a combination of climate factors, such as wind speeds, temperature, precipitation, and soil factors such as surface terrain roughness, and vegetation coverage. The Wind Erosion Equation (WEQ) published by Woodruff and Siddoway (1965), models this phenomenon. The Revised Wind Equation (RWEQ) extends the WEQ by utilizing wind as the primary factor rather than soil erodibility as WEQ does. Fryrear et al. (2001) show that RWEQ is a much more accurate model: the correlation between measured erosion and estimated erosion with WEQ was not significant ($r^2 = 0.01$), whereas the correlation with RWEQ was highly significant ($r^2 = 0.927$) (Fryrear, 2001). RWEQ also takes soil surface roughness into account unlike WEQ.

We used the RWEQ model to estimate wind erosion in the Gobi Steppe. In East Asia, the Gobi Steppe is a region sensitive to global climate change, due to degraded grasslands and deserted croplands (Hu, 2003); where dust storms are regarded as one of the most severe environmental problems (Qi, 2010). Our area of interest specifically is the Eastern Gobi Steppe.

Closer to the Eastern Gobi Steppe, in the Inner Mongolia Province of China, wind erosion had been simulated using RWEQ by Jiang et. Al (2016), where they have shown that there is high correlation ($r^2 = 0.88$) between RWEQ estimates of wind erosion and measurements obtained from remote sensing data (Jiang, 2016). They find that 23.2% of this erosion could be rated as severe between 2001 and 2010 (Jiang, 2016). Corroborating these findings, Haiyan (2018) finds that 23.2% of the wind erosion can be rated as severe from 1990 to 2015, also using RWEQ-based models. Other approaches result in more variability - e.g., Qi (2010) finds annual soil erosion rates ranging from 53.12 t/km² to 479.63 t/km² over 8 sampling sites, using the Cs tracing technique (Fulajtár et al., 2017) which analyzes changes of 137-Caesium, which is found bound to soil colloids, inventories in soil to measure soil erosion on 8 sampling sites in the Mongolian Plateau; Shi (2009) finds a categorical map of wind erosion across the Mongolian Plateau, ranking wind erosion from none to severe, using a fuzzy c-means clustering technique which is an automatic classification method that expresses gradual spatial changes of physical geographic phenomena, such as wind erosion in this case, by using a continuously divided membership model (Shi, 2009). A more recent study utilized RWEQ in Inner Mongolia to calculate soil loss and categorize it according to standards of the Ministry of Water Resources of China, and analyzed the migration paths of the erosion, finding that "Tolerable and slight aeolian erosion intensities characterized most of Inner Mongolia's area, being widely distributed across the region, while moderate intensity was mainly clustered in its southwest and southeast" and that "the SL's maximum, minimum, and mean values sharply decreased prior to 2013 but they increased later" (Dai, 2022). Another recent study utilized RWEQ to calculate wind erosion in Inner Mongolia, finding that wind erosion intensity in many regions increased from light to mild and moderate, with the area and intensity of soil wind erosion displaying an increasing trend (Lyu, 2021). Though RWEQ has been validated in these areas surrounding the Eastern Gobi Steppe, no ground truth measurement are available, to date, in the Eastern Gobi Steppe itself.[WCG2][DT3]

The Chinese government implemented measures to prevent sandstorms and wind erosion via the Beijing-Tianjin Sandstorm Source Control Project to be implemented from 2013 to 2022. ("Counties Benefit from Beijing-Tianjin Sandstorm Source Control Project", 2020). This project is focused on the Chinese provinces of Beijing, Tianjin, Hebei, Shanxi, Shaanxi and Inner Mongolia. In this project, resources are invested into afforestation, sand fixation, and degraded shelter forest reconstruction. Afforestation, the planting of new trees, and forest reconstruction increase vegetation coverage significantly. The benefits of this project are widespread. For example, the income of farmers and herdsmen in the area

has been increased, and the more stable ecosystem bolstered by the increase in vegetation coverage will contribute to conservation of animal and plant species.

Though wind erosion has been estimated in the Inner Mongolia Province in China, by Jiang et. al. (2016) and Haiyan et. al. (2018), estimates are missing for the Eastern Gobi Steppe. Based on the strong correlation of RWEQ estimates against wind erosion measurements shown by Fryrear et. al. (2001) and Jiang et. al. (2016), we aim here to use a RWEQ-based model to estimate wind erosion in the Mongolian Gobi Steppe and most importantly understand its main drivers. This allows us to simulate wind erosion under possible future scenarios of climate and vegetation cover. This work also outputs a replicable implementation of the RWEQ-based wind erosion model, globally applicable with data at various resolutions.

1.1. The Eastern Gobi Steppe

The Eastern Gobi Steppe stretches from the Inner Mongolia Plateau in China into Mongolia at 1,000 to 1,500 m elevation, northward into Mongolia. Summer heat depends on elevation, ranging from warm to hot, and winters are severely cold. Winter conditions are harsher here than other parts of China at similar altitudes and latitudes, as there are no mountains to shelter the region from northerly winds. Annual total precipitation varies significantly, and most of the precipitation is in summer. Vegetation consists of drought-resistant shrubs and low grasses.

Our study area, an area of 69.3 * 10^3 km^2, where sensitivity analysis was conducted, is located along Mongolia's southern border and inside the Gobi desert. This area is characterized by extremely low rainfall and very little vegetation cover (Martin et al., 2022). The mean temperature is 3.7°C annually, with a maximum of 31.5°C and a minimum of -23.2°C. Annual precipitation is 100 to 150 mm, and most rainfall occurs in summer (Magsar, 2018).

We used the RWEQ model to estimate wind erosion in one region of the Mongolian Plateau (Figure 1). In East Asia, the Mongolian Plateau is a region sensitive to global climate change; where dust storms are regarded as one of the most severe environmental problems (Qi, 2010). We conducted a sensitivity analysis of the RWEQ model in a portion of the Eastern Gobi Steppe, outlined in the map with a red border, to analyze which environmental factors have the greatest influence in predicting wind erosion. The results of the analysis are detailed in further sections of this paper.

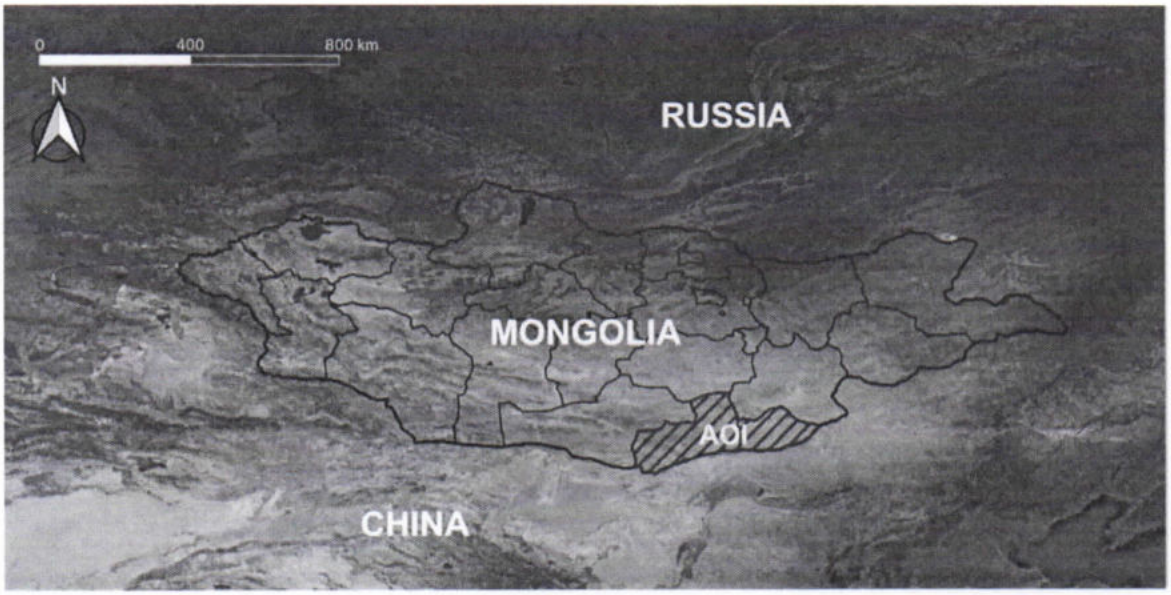

Figure 1. Map of our Area Of Interest (AOI) in Mongolia. Borders overlayed on Google Earth satellite basemap.

2. METHODS

2.1. RWEQ Model

The RWEQ model estimates Soil Loss (SL) for a given location. Weather, soil erodibility, soil crust, surface terrain roughness and vegetation coverage factors are used to calculate the maximum transported capacity by wind (Qmax) and the critical field length (S) as shown below (Visser, 2005; Jarrah, 2020):

$$Qmax = 109.8 * (WF * EF * K' * SCF * COG) \quad (1)$$

$$S = 150.71 * (WF * EF * K' * SCF * COG)^{-0.3711} \quad (2)$$

$$SL = 100/(S^2 + 0.01) * Qmax * (e^{-(50 / (S + 0.01))})^2 \quad (3)$$

where Qmax (in kg/m) is the transport capacity and S (in m) is the distance where 63% of the maximum transport capacity is reached, called the critical field length. SL (in kg/m^2) is the rate of soil loss caused by wind erosion (Z from the original equation is 50 here, and is already factored in). WF is the Weather Factor, SCF is the Soil Crusting Factor, EF is the soil Erodible Fraction, COG is the vegetation factor, and K' is the surface terrain roughness factor.

Weather Factor (WF, in kg m^{-1}). Wind is the cornerstone of RWEQ, with soil moisture and snow cover as important factors influencing wind erosion. In this paper, the weather factor is calculated on a monthly basis. The weather factor represents the effect of climate on wind erosion, and combines wind speed, soil moisture, and snow cover as shown below:

$$WF_{monthly} = Wf * \rho / 9.8 * SW * SD \quad (4)$$

where WF is the weather factor (in kg/m), Wf is the wind factor (in m^3/s^3), ϱ is air density (in kg/m^3), 9.8 is acceleration due to gravity (in m/s^2), SW represents soil moisture, and SD represents snow cover.

The wind factor is calculated from daily wind speed (ws, in m/s) using the equation shown below (Jarrah, 2020) when the wind speed value is higher than the threshold of 5 m/s. For all wind speed values less than this threshold, the wind factor is equal to 0 (Stetler, 1997):

$$Wf = ws * (ws - 5)^2 \quad (5)$$

The soil moisture factor is calculated from monthly potential evapotranspiration (ETp, in mm), monthly total precipitation (PRCP, in mm), monthly number of rainy days (PRCP_DAYS) as shown below (Jarrah, 2020):

$$SW = (ETp - PRCP * PRCP\_DAYS) / ETp \quad (6)$$

Monthly potential evapotranspiration is calculated from monthly total solar radiation (SOL, in MJ/m^2) and monthly average temperature (TEMP, in °C) as shown (Samani & Pessarakli, 1985):

$$ETp = 0.0135 * (SOL / 2.54) * (TEMP + 17.8) \quad (7)$$

SD is the snow cover factor determined as 1 – probability of snow depth > 25.4 mm (Jarrah, 2020).

Soil Crusting Factor (SCF). When rain hits the soil surface, there is a formation of surface crust because of redistributed soil particles. That soil surface can be hard or weak and may affect wind erosion potential (Jiang, 2016). The soil crusting factor is a non-temporal value calculated from clay (CL, %) and organic matter (OM, %) as shown below (Jiang, 2016):

$$SCF = 1 / (1 + 0.0066 * CL^2 + 0.021 * OM^2) \quad (8)$$

Soil Erodible Fraction (EF). The erodible fraction is the fraction of the surface 25 mm of soil that is lower than 0.84 mm in diameter as determined by a standard compact rotary sieve, and the highest value of EF for a year is related to the physical and chemical properties of the soil (Jiang, 2016) The erodible fraction is a non-temporal value calculated

from the ratios of sand (SND, %), silt (SILT, %), clay (CL, %), and organic matter (OM, %) in the soil as shown in the following equation (Jarrah, 2020):

$$EF = (29.09 + 0.31 * SND + 0.17 * SILT + 0.33 * SND / CL - 2.59 * OM - 0.95 * 0) / 100$$ (9)

Vegetation factor (COG). The amount of vegetation coverage over the soil can have a significant impact on how well the soil is protected from erosion. The monthly vegetation factor can be calculated from the monthly fraction of vegetation coverage (FVC, %) as shown in the following equation (Jarrah, 2020):

$$COG = e^{(-0.00438 * FVC)}$$ (10)

The original equation has additional factors as shown (Jarrah, 2020). However, due to limited availability of data, only the term related to FVC was used. This was based on the work done by Jiang (2016) in the same geographical region:

$$COG = e^{(-0.00438 * FVC)} + e^{(-0.0344 SA^{0.6413})} + e^{(5.614 CC^{0.7366})}$$ (11)

where FVC is the percent of land covered by crop residue, SA is the standing stem area index and CC is the percent soil surface covered by crop canopy.

Surface terrain roughness factor (K'). Surface terrain roughness is calculated on a monthly basis from topographical roughness (Kr) and the Chain Random Roughness (Crr), a measure of surface roughness via the chain method (Saleh, 1993), as shown in the following equation (Jiang, 2016):

$$K' = e^{(1.86 * Kr - 2.41 * Kr^{0.934} - 0.127 Crr)}$$ (12)

Topographical roughness is calculated for 3x3 grid of pixels of the raster data from the difference between the minimum and maximum elevations in the selected area (H, in m) and the length of the edge of the area (L = 3 * resolution of raster) in the following equation (Jiang, 2016):

$$Kr = 0.2 * (H^2 / L)$$ (13)

Chain random roughness is calculated from the monthly fraction of vegetation coverage (FVC) fraction) as shown in the following relationships. It is computed in two steps. First, a random roughness is computed from FVC (Zhibao, 1996). Then the computed random roughness is used to calculate chain random roughness (Borelli, 2016):

$$RR = 0.025 + 2.464 FVC^{3.56}$$ (14)

$$Crr = 17.46 * (RR)^{0.738} \quad (15)$$ 214

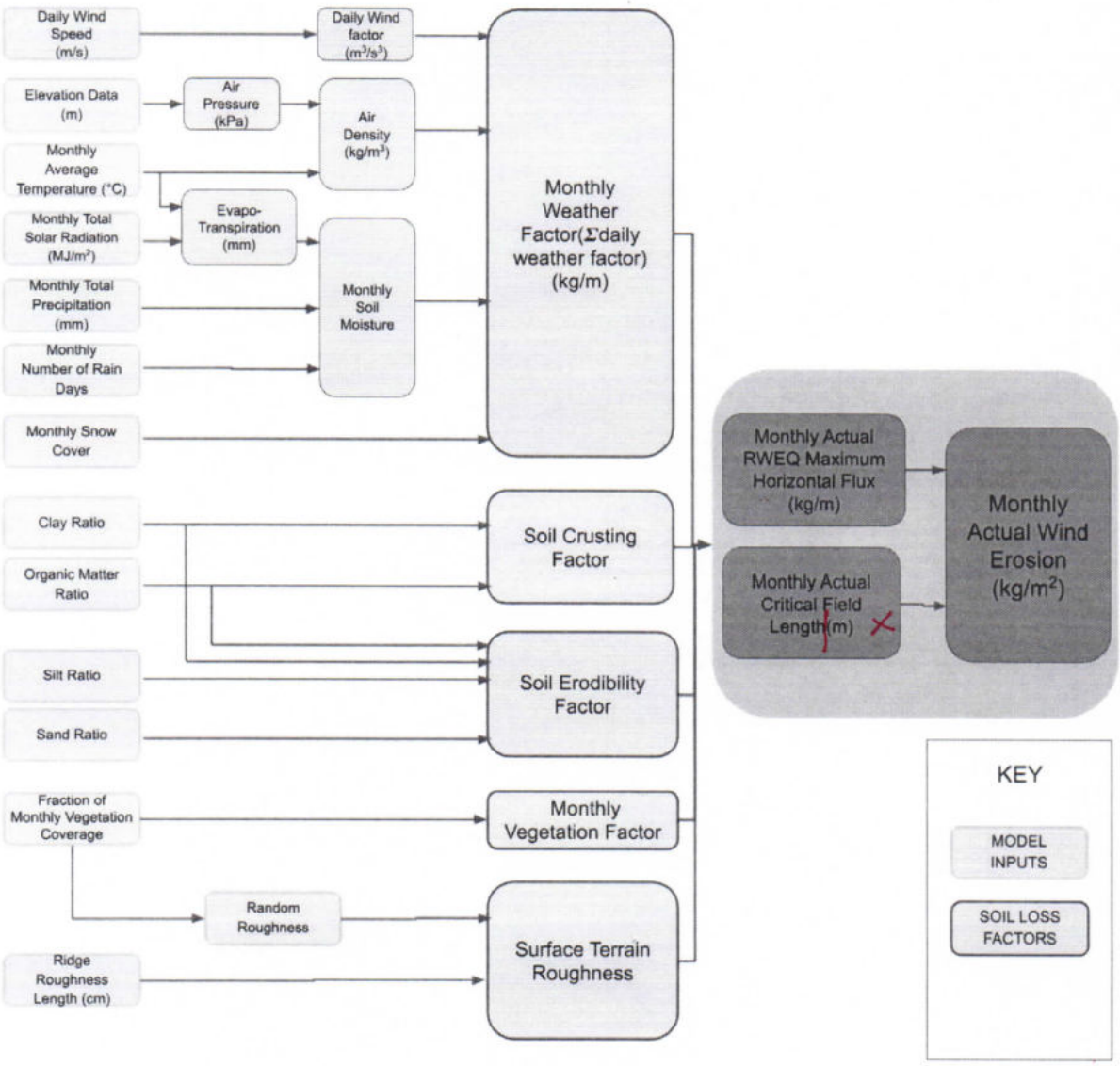

Figure 2. Model flowchart summary. Demonstrates how inputs are utilized to calculate factors used for final soil loss calculation. 215 216

2.2. *Input Data Sources* 217

The Digital Elevation Model (DEM) data is downloaded from the Shuttle Radar Topography Mission (SRTM) website for the country of Mongolia (Survey, 2020). Wind speed is sourced from the ERA5-Land Dataset on the Copernicus Climate Data Store (Muñoz, 2019). Monthly average temperature and total precipitation come directly from Worldclim current conditions (Fick, 2017). Solar radiation is calculated according to Penman (1948). Precipitation days information from a public website is used (Amicus Travel, 2020). To justify the use of this website, the data was compared to Climate Hazards Group InfraRed Precipitation with Station data (CHIRPS), and found to be only 1 or 2 days apart. As varying number of rain days was shown to have almost no impact on wind erosion results based on the sensitivity analyses, the travel website data served as a reasonable 218 219 220 221 222 223 224 225 226 227

source of the number of rain days. Clay, silt, and sand fractions are from ISRIC SoilGrids 250_m (Hengl, 2017). Soil organic matter and monthly snow cover are outputs of the Rangeland Production model (Kowal et al., 2021), driven by Worldclim historical vegetation. Monthly herbaceous vegetation cover is calculated from herbaceous biomass outputs from the Rangeland Production Model, and a simple linear regression relating standing biomass to vegetation cover estimated from vegetation collected in the study area as described by Ahlborn (Ahlborn, 2020). The temporal inputs are collected on a monthly basis, excepting wind speed, which is a daily data value, that is used to calculate a total monthly wind factor. Due to the differences in resolution of each of our input data sources, each GeoTiff file was scaled to the resolution of the elevation file with Python, averaging values for groups of pixels for higher resolution data.

Table 1: Data collection. This table summarizes the data used for this paper, including the source, unit, original resolution and format.

Category	Dataset	Source	Temporal Range (Year)	Unit	Original Resolution	Format
Elevation	Elevation Data (DEM)	SRTM	2000	m	0.05985 degrees^2[DT4] per pixel	GeoTIF
Climate	Monthly Average Temperature	Worldclim current conditions	1970–2000	°C	0.00833 degrees^2 per pixel	GeoTIF
	Monthly Total Precipitation	Worldclim current conditions	1970–2000	mm	0.00833 degrees^2 per pixel	GeoTIF
	Monthly Solar Radiation	Rangeland Production Model Output	2014-2015	MJ/m^2	0.00324 degrees^2 per pixel	GeoTIF
	Monthly Snow Cover	Rangeland Production Model Output	2014-2015	% (probability)	0.05003 degrees^2 per pixel	GeoTIF
	Monthly	Amicus	2020	day	0.05985 degrees^2 per	GeoTIF

The other three scenarios use 110%, 120%, and 150% of the original values for each pixel. Soil loss maps are generated for each month and then summed temporally to generate annual soil loss maps for visual comparison.

Another sensitivity analysis is done by computing the percentage change of the annual soil loss compared to the actual annual soil loss at the maximum and minimum values for each model input. The computation is done by setting only one input to the maximum or minimum at a time. For each analysis, each pixel in the area of interest for the selected input parameter is set uniformly to the maximum or minimum value. The soil loss is summed temporally as well as spatially to have a single value representation of the scaling effect for each parameter. Results are captured in Table 3 [DT5]for comparison.

3. RESULTS AND DISCUSSION

3.1. Model results in Eastern Gobi Steppe

Results from our model are consistent with previous studies done in the same area.

A RWEQ-based wind erosion analysis has been done over the Inner Mongolia province of China (Haiyan, 2018). The equations are identical, excepting the equation for potential evapotranspiration. Our coefficient that multiples solar radiation and temperature after combining the numerical factors in the equation is 0.00531, while the Haiyan coefficient is 0.000277. Our equation to calculate potential Evapotranspiration (ETp) was derived from Samani & Pessarakli (1985). After comparison, it is found that the ETp values are consistent and the differences in equation would not affect the correctness of final results. Our area of interest, the Eastern Mongolian Steppe, overlaps part of the region covered by their study. That paper categorized wind erosion into different classes of severity from tolerable to destructive. A visual comparison of their figures shows that overlapping area falls into the Severe and Very Severe categories. According to Haiyan (2018), the Severe category has a soil erosion range of 5000 to 8000 t/km²/a and the Very Severe category has a soil erosion range of 8000 to 15000 t/km²/a. Our estimated total soil erosion was $61 * 10^{10}$ kg over an area of $69.3 * 10^{9}$ m² which corresponds to 8800 t/km². To give a comparison, that amount of soil loss for an area of the size of the city San Francisco would be 3 elephants in weight. [WCG6][DT7] Considering that the bulk density of fine soil that is transported in wind erosion is 1500 kg/m³, the average thickness of soil transported in a square kilometer is about 0.5 cm (Du Plessis & Van Huyssteen, 2019). Realistically, not all the total area will be eroded by the wind, because the transported soil can accumulate in certain locations, e.g., in the surroundings of a windbreak, a vegetation patch, or in a ditch. This shows that the results of this study are consistent with prior published results in the overlapping areas of Inner Mongolia.

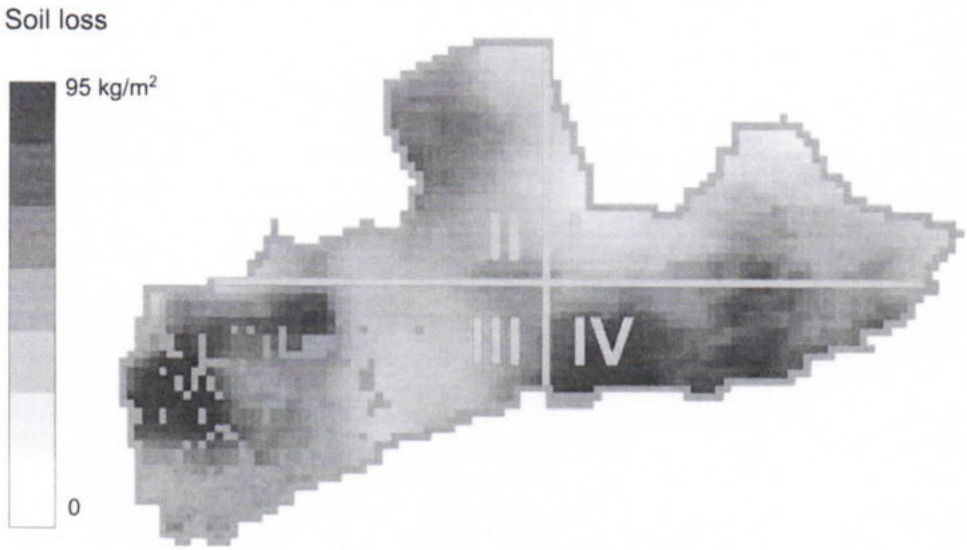

Figure 3. Map of annual soil erosion in our area of interest split into four quadrants. For each quadrant, the spatial maximum and minimum soil erosion will be represented as categories according to Haiyan (2018).

Table 2: Data comparison. This table summarizes the categories of severity of wind erosion from Haiyan (2018) and compares them with our annual wind erosions based on each quadrant of the area of interest (Figure 3)

Area	Erosion level as defined by Haiyan (2018) (t/km²)	Annual wind erosion, as calculated in this study (t/km²)
Total Soil Loss / Total Area	Very Severe (8000 - 15000)	8800
Quadrant I (North East)	Moderate (2500 - 5000) - Destructive (> 15000)	2600 - 63000
Quadrant II (North West)	Very Severe (8000 - 15000) - Destructive (> 15000)	8900 - 69000
Quadrant III (South West)	Very Severe (8000 - 15000) - Destructive (> 15000)	8200 - 93000
Quadrant IV (South East)	Destructive (> 15000) - Destructive (> 15000)	21000 - 95000

The Eastern Gobi Steppe Area has almost double the soil loss per unit area of Inner Mongolia because it is less vegetated.

Our model estimates the total annual soil loss for the Mongolian Eastern Gobi Steppe to be 0.61 * 10^9 t. Another study on soil loss in Inner Mongolia of China, a nearby region, estimates the annual soil losses to be in the range of 4 to 5.7 billion tonnes (Jiang, 2016). In comparison, our model estimates the total annual soil loss for the Mongolian Eastern Gobi Steppe to be 0.61 * 10^9 t (61 * 10^{10} kg). The area of interest in that study is 1.2 million km², whereas our area of interest has an area of 69300 km². Comparing these numbers, we see that the Eastern Gobi Steppe Area has almost double the soil loss per unit area of Inner Mongolia. This is because the Inner Mongolia area of interest is larger and contains areas with a large range of vegetation coverage, so there is less wind erosion on average due to the influence of vegetation-heavy areas, which are not present in the Eastern Gobi Steppe.

3.2. *Environmental Factors Contributing to Soil Loss*

3.2.1. Impact of five primary RWEQ factors

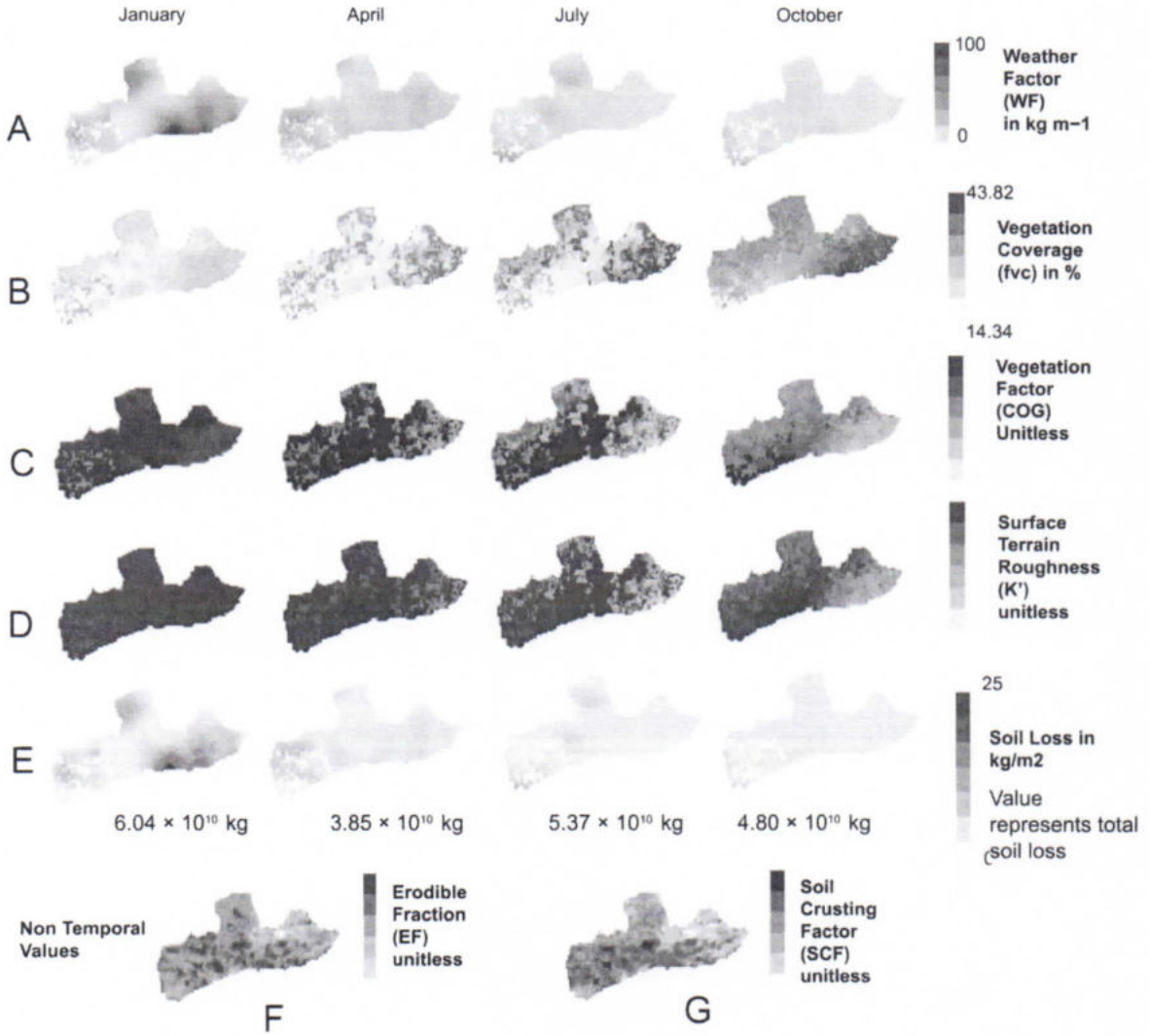

Figure 4. Soil loss factors per season. Inputs are monthly, this figure highlights one month per season.

Soil erosion is affected by the seasonal variation of the weather factor and vegetation coverage.

RWEQ's primary factors are Weather Factor (WF), vegetation factor (COG), Surface Terrain Roughness (K'), Erodible Fraction (EF), and Soil Crusting Factor (SCF). Figure 4 displays maps of each of these five primary factors, along with the estimated soil loss, for our area of interest. Though the spatial distribution of each factor varies across months, we have chosen four months, January, April, July, and October to represent the four seasons. In addition to the primary factors, fractional vegetation coverage maps are shown to highlight the relation between seasonal soil loss and vegetation coverage. The weather factor represents the effect of climate on wind erosion, and combines wind speed, soil moisture, and snow cover. As shown in Figure 4-A and 4-E, the higher weather factor in January leads to a higher soil loss for the month. Figure 4-C also shows that COG is high for January. COG is inverse to fractional vegetation coverage, which implies lower vegetation coverage. Indeed, the fractional vegetation coverage in January is the lowest of the four seasons which contributes to the high soil loss in that month. Increased wind speeds caused increased soil erosion. Whereas increased soil moisture, vegetation, and snow cover decrease wind sensitivity. Thus, these factors must be lower for wind to cause severe soil loss. The lower levels of vegetation coverage corroborate this conclusion. In October, the low weather factor and high fractional vegetation coverage boost each other's effect in decreasing wind sensitivity, resulting in comparatively lower soil loss in that month. K' shows similar variability across the seasons as COG since both factors are dependent on fractional vegetation coverage. Any impact of cultivation practices on K' was not taken into account in this study due to lack of data. The seasonal variation of SCF and EF is not expected in this region and this project used non-temporally variable soil composition data.

3.2.2. Sensitivity of Soil Loss

An introductory text should be written here

Figure 5. Plots of Sensitivity of Soil Loss to Model Inputs. The sensitivity of soil loss was plotted against scenarios of 0%, 50%, 100%, and original vegetation coverage. The y-axis represents soil loss in kg/m² and the x-axis represents the scale parameter that multiplies the input (e.g., 0.5 for 50%)

This should be displaced below the figure

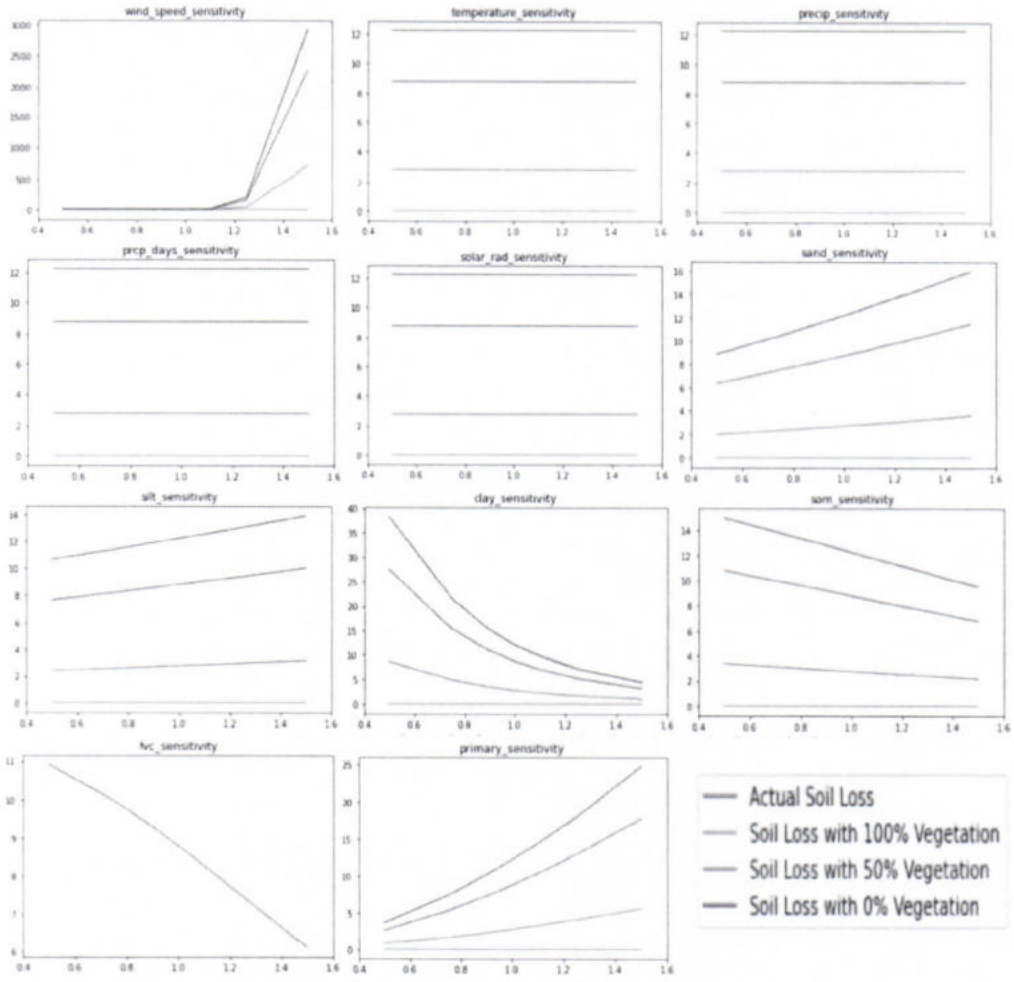

Too small letters and numbers!

Figure 5.

Table 3. Sensitivity analysis of Soil Loss (SL) against model inputs. Sensitivity is measured as the perfect change in the annual, spatial soil loss sum if an input is increased or decreased by a percentage of the original value, or uniformly set to the minimum or maximum value of the spatial data. The actual annual soil loss rate is 8800 t/km^2.

Note 1: The sensitivity analysis for the soil loss factors (WF, SCF, EF, KPRIME, COG) is done by applying a single scale factor to the product of these factors in the RWEQ model for maximum transported capacity by wind (Qmax) and the critical field length (S). As such, there is no representative min or max value that could be used.

Variable	Affected Soil Loss Factors	Global Average of Variable	Global Range {min - max}	Maximum Spatial Range {min - max}	Maximum Seasonal Range {min - max}	SL sum (%) difference with variable=50 % of actual value	SL sum (%) difference with variable=150 % of actual value	SL sum (%) diff when variable=min of Global Range uniformly	SL sum (%) diff when variable=max of Global Range

This observation is more pronounced when all spatio-temporal wind speed values are increased by 150%. As most of the wind speed values are between 3 m/s and 5 m/s, a 150% increase makes many of them higher than the threshold and contributes to the soil loss. In addition, the wind speed has a cubic relation to the weather factor, so a small increase in non-zero entries of wind speed values results in significantly higher weather factor, hence, soil loss. This is in line with the general principle of RWEQ's reliance on wind as a cornerstone (Fryrear, 2001).

Fractional vegetation and clay ratio are the most significant soil-based factors.

The soil parameters (sand, silt, clay, organic matter) also have significant effects on soil loss (Table 3); in particular, the clay ratio especially affects soil loss as higher clay in the soil allows it to maintain larger clumps which could reduce the impact of wind erosion (Purdue). Similarly, fractional vegetation coverage also has a significant effect on soil loss.

Precipitation and solar radiation are not as significant.

The results show a lack of sensitivity of soil loss to precipitation, number of rain days, and solar radiation as shown by the less than 10% change in the corresponding rows of Table 3. With a range of only 0 to 47 ~~millimeters~~ m.m.s of rain both spatially and temporally, the low sensitivity may be a result of low precipitation (Table 3). The difference in sensitivity between these factors is displayed even more clearly in the plots of Figure 5, where there are steep changes in the plot for factors such as wind speed , and flatter lines for precipitation and solar radiation.

3.3. Impact of Vegetation Coverage

3.3.1. Effect of Vegetation Coverage on Soil Loss

Increasing vegetation coverage significantly reduces wind erosion.

Vegetation coverage has a significant impact on soil loss, as observed by the soil loss percent change with varying magnitudes of fractional vegetation coverage (Figure 5). The areas with minimal vegetation coverage (Map B) result in more soil loss (Map A), such as the western side of the area of interest. At fractional vegetation coverage in the range of 30% to 50%, the soil loss is in the range of 0.001 kg/m^2 to 0.002 kg/m^2 as shown in the eastern side of the area in Maps A and B. A potential soil loss estimation with 0% Fractional Vegetation Coverage (FVC) shows more soil loss as shown in Map C. Specifically, the eastern side shows higher percent change in soil loss in the range of 70% to 100% (Map C). This is consistent with the higher FVC in that area (Map B) where the soil loss is minimized by the higher vegetation coverage. If that coverage is removed, the area becomes susceptible to higher soil loss. On the other hand, the theoretical scenarios where FVC is uniformly 50% (Map D) and 100% (Map E) indicate that soil loss could be significantly reduced with substantially increased vegetation. Soil loss would decrease by 60% to 80% with 50% FVC and decrease by 90% to 100% with 100% FVC. If the vegetation coverage in each area is increased to 110% (Map F), 120% (Map G), or 150% (Map H) of the original vegetation coverage, it results in reduced soil loss to a lesser degree, from 20% to 60% decrease.

Figure 21. Monthly Surface Terrain Roughness (K').

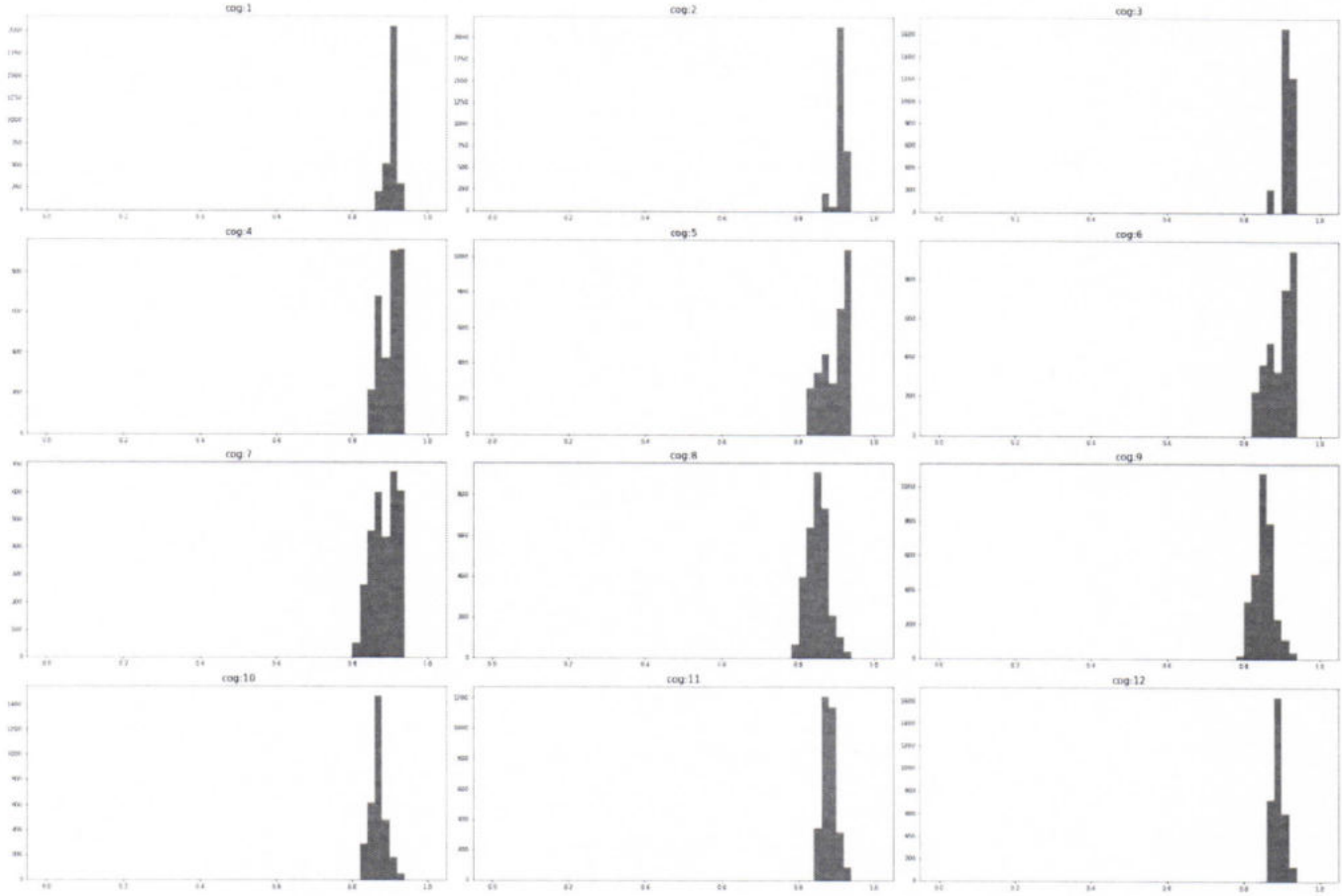

Figure 22. Monthly Vegetation Factor (COG).

Supplementary Materials: The following supporting information can be downloaded at: www.mdpi.com/xxx/s1, Figure S1: title; Table S1: title; Video S1: title.

Author Contributions: Conceptualization, Charlotte Weil; Data curation, Charlotte Weil, Binbin Huang and Virginia Anne Kowal; Investigation, Isita Nandana Talukdar; Methodology, Isita Nandana Talukdar; Project administration, Charlotte Weil; Software, Isita Nandana Talukdar and Binbin Huang; Supervision, Charlotte Weil; Validation, Isita Nandana Talukdar; Writing – original draft, Isita Nandana Talukdar; Writing – review & editing, Charlotte Weil, Binbin Huang and Virginia Anne Kowal.

Funding: This work was supported by the NASA Biodiversity and Ecological Forecasting Program, Award Number NNX17AG56G

Data Availability Statement: The input data used is available as sample data in this repository: https://github.com/charlottegiseleweil/winderosion. Following the usage example in the README will generate the wind erosion outputs used in this study.

Acknowledgments: The authors would like to thank Dr. Rebecca Chaplin-Kramer, who inspired this work, made it possible and was of great advice all along.

References

1. Ahlborn, J., von Wehrden, H., Lang, B., Römermann, C., Oyunbileg, M., Oyuntsetseg, B., & Wesche, K. (2020). Climate–grazing interactions in Mongolian rangelands: Effects of grazing change along a large-scale environmental gradient. Journal of Arid Environments, 173, 104043.
2. Amicus Travel. (2020, January 02). GOBI DESERT CLIMATE: Average monthly temperature and weather. Retrieved September 01, 2020, from https://www.amicusmongolia.com/climate-average-monthly-temperature-weather-gobi-desert-mongolia.html
3. Borrelli, P., Lugato, E., Montanarella, L., & Panagos, P. (2016). A New Assessment of Soil Loss Due to Wind Erosion in European Agricultural Soils Using a Quantitative Spatially Distributed Modelling Approach. Land Degradation & Development. 28. 10.1002/ldr.2588.
4. Buschiazzo, D. E., & Zobeck, T. M. (2008). Validation of WEQ, RWEQ and WEPS wind erosion for different arable land management systems in the Argentinean Pampas. Earth Surface Processes and Landforms, 33(12), 1839–1850. https://doi.org/10.1002/esp.1738.
5. Calkins, K. (2005). Correlation Coefficients. Andrews.edu. Retrieved 9 November 2021, from https://www.andrews.edu/~calkins/math/edrm611/edrm05.htm.
6. Counties Benefit from Beijing-Tianjin Sandstorm Source Control Project. China Global Television Network News. (2020, September 27). Retrieved 9 November 2021, from https://news.cgtn.com/news/2020-09-27/Counties-benefit-from-Beijing-Tianjin-sandstorm-source-control-project-U7wvmur4Zy/index.html.
7. Dai, Y., Tian, L., Zhu P., Dong Z., Zhang R. Dynamic aeolian erosion evaluation and ecological service assessment in Inner Mongolia, northern China, Geoderma, Volume 406, 2022, 115518, ISSN 0016-7061, https://doi.org/10.1016/j.geoderma.2021.115518.
8. Dong, Z., Chen, W., Li Z., Yang Z.. The laboratory Study on the Role of Vegetation in Soil Erosion by Wind [J] Journal of Soil Erosion and Soil and Water Conservation. 1996, 002(002):1-8. (In Chinese)
9. Dou, X., Ma, X., Zhao, C., Li, J., Yan, Y., Zhu, J., Risk assessment of soil erosion in Central Asia under global warming, CATENA, Volume 212, 2022, 106056, ISSN 0341-8162, https://doi.org/10.1016/j.catena.2022.106056.
10. Duniway, M. C., Pfennigwerth, A. A., Fick, S. E., Nauman, T. W., Belnap, J., & Barger, N. N. (2019). Wind erosion and dust from US drylands: a review of causes, consequences, and solutions in a changing world. Ecosphere, 10(3), e02650.
11. Du Plessis, M., & Van Huyssteen, C. (2019). *Soil: The producer's most important asset part 5: Physical properties of soil*. Grain SA Home. Retrieved June 14, 2022, from https://www.grainsa.co.za/soil-the-producers-most-important-asset--part-5-physical-properties-of-soil?print=1#:~:text=Bulk%20density&text=It%20is%20usually%20expressed%20as,1%20300%20kg%2Fm3.
12. Engineering ToolBox, (2003). Atmospheric Pressure vs. Elevation above Sea Level. [online] Available at: https://www.engineeringtoolbox.com/air-altitude-pressure-d_462.html [Accessed August, 30, 2020]].
13. Fick, S. E., & Hijmans, R.J. (2017). WorldClim 2: new 1 km spatial resolution climate surfaces for global land areas. International Journal of Climatology 37 (12): 4302-4315; available from worldclim.org.
14. Fryrear, D., Sutherland, P., Davis, G., Hardee, G., & Dollar, M. (2001). Wind erosion estimates with RWEQ and WEQ. COKS Assembly St. 67401.
15. Fu, B., Liu, Y., Lü, Y., He, C., Zeng, Y., & Wu, B. (2011). Assessing the soil erosion control service of ecosystems change in the Loess Plateau of China. Ecological Complexity, 8(4), 284–293. https://doi.org/10.1016/j.ecocom.2011.07.003
16. Fulajtár, E., Mabit, L., Renschler, C. S., & Zhi, Y. A. L. (2017). Use of ^{137}cs for soil erosion assessment / Fulajtár, E., Mabit, L., Renschler, C. S., & Zhi, Y. A. L.. Food and Agriculture Organization of the United Nations, International Atomic Energy Agency.
17. Griffin, D. W. (2007). Atmospheric movement of microorganisms in clouds of desert dust and implications for human health. Clinical Microbiology Reviews, 20(3), 459–477. https://doi.org/10.1128/CMR.00039-06.
18. Haiyan, Z., Fan, L., Cao, W., Harris, W., Yuzhe, L., Chi, W., Wang, S.. (2018). Response of wind erosion dynamics to climate change and human activity in Inner Mongolia, China during 1990 to 2015. Science of the Total Environment. 639. 1038-1050. 10.1016/j.scitotenv.2018.05.082.
19. Hengl, T., Mendes de Jesus, J., Heuvelink, G. B., Ruiperez Gonzalez, M., Kilibarda, M., Blagotić, A., ... & Guevara, M. A. (2017). SoilGrids250m: Global gridded soil information based on machine learning. PLoS one, 12(2), e0169748
20. Hu Y., Liu J., Zhuang D., Yang F. Study on the Relationship Between Land-use Dynamics and WindErosion Dynamics in Inner Mongolia During Late 1990s[J]. Progress In Geography, 2003, 22(6): 541-550.
21. Jarrah, M., Mayel, S., Tatarko, J., Funk, R., & Kuka, K. (2020). A review of wind erosion models: Data requirements, processes, and validity. Catena, 187, 104388.
22. Jiang, L., Xiao, Y., Zheng, H. et al. Spatio-temporal variation of wind erosion in Inner Mongolia of China between 2001 and 2010. Chin. Geogr. Sci. 26, 155–164 (2016). https://doi.org/10.1007/s11769-016-0797-y.
23. Joshi, J. R., Quantifying the impact of cropland wind erosion on air quality: A high-resolution modeling case study of an Arizona dust storm, Atmospheric Environment, Volume 263, 2021, 118658, ISSN 1352-2310, https://doi.org/10.1016/j.atmosenv.2021.118658.
24. Kowal, V., Ahlborn, J., Jamsranjav, C., Avirmed, O., & Chaplin-Kramer, R. (2021). Modeling Integrated Impacts of Climate Change and Grazing on Mongolia's Rangelands. Land, 10(4), 397. MDPI AG. Retrieved from http://dx.doi.org/10.3390/land10040397.

25. Lacková, L.; Pokrývková, J.; Kozlovsky Dufková, J.; Policht-Latawiec, A.; Michałowska, K.; Dąbrowska, J. Long-Term Impact of Wind Erosion on the Particle Size Distribution of Soils in the Eastern Part of the European Union. *Entropy* 2021, *23*, 935. https://doi.org/10.3390/e23080935.
26. Li, H., Gao, H., Feng, X., Wang, X., & Du, B. (2005). Contribution of farmland wind erosion to sand storms in northern China. In Remote Sensing and Modeling of Ecosystems for Sustainability II (Vol. 5884, p. 58840L). International Society for Optics and Photonics.
27. Lyu, X., Li, X., Wang, H., Gong, J., Li, S., Dou, H., & Dang, D. (2021). Soil wind erosion evaluation and sustainable management of typical steppe in Inner Mongolia, China. *Journal of environmental management*, *277*, 111488. https://doi.org/10.1016/j.jenvman.2020.111488.
28. Magsar, U., Baasansuren, E., Tovuudorj, ME. *et al.* Medicinal plant diversity in the southern and eastern Gobi Desert region, Mongolia. *J Ecology Environ* 42, 4 (2018). https://doi.org/10.1186/s41610-018-0064-5
29. Martin, E., Mattison, E., Taylor, K., Cripps, L., Lima, M., & Maney, C. (2022). *Eastern gobi desert steppe*. Eastern Gobi Desert Steppe. Retrieved June 14, 2022, from https://www.oneearth.org/ecoregions/eastern-gobi-desert-steppe/.
30. Muñoz Sabater, J., (2019): ERA5-Land hourly data from 1981 to present. Copernicus Climate Change Service (C3S) Climate Data Store (CDS). (Accessed on < 20-09-2020 >), 10.24381/cds.e2161bac.
31. Penman, H. L. (1948). Natural evaporation from open water, bare soil and grass. Proceedings of the Royal Society of London. Series A. Mathematical and Physical Sciences, 193(1032), 120-145.
32. Purdue University. Soil Erosion by Wind. Retrieved September 21, 2020, from https://www.agry.purdue.edu/soils_judging/new_manual/ch6-wind.html.
33. Qi, Y., Liu, J., Shi, H., Zhuang, D., & Hu, Y. (2010). Estimation of wind erosion rates of Mongolian Plateau by using 137 Cs tracing technique.
34. Saleh, A. 1993. Soil roughness measurement: Chain method. J. Soil Water Cons. 48(6): 527- 529.
35. Samani, Z. A., Pessarakli, M., (1986). Estimating Potential Crop Evapotranspiration with Minimum Data in Arizona. In Transactions of the ASAE (Vol. 29, Issue 2, pp. 0522–0524). American Society of Agricultural and Biological Engineers (ASABE). https://doi.org/10.13031/2013.30184
36. Saxton, K., Chandler, D., Schillinger, W. (2001). Wind erosion and air quality research in the northwest US Columbia Plateau: Organization and progress. In The 10th International Soil Conservation Organization Meeting (pp. 766-770).
37. Shi, H., Gao, Q., Qi, Y., Liu, J., Hu, Y., (2009). Wind erosion hazard assessment of the Mongolian Plateau using FCM and GIS techniques. Environmental Earth Sciences. 61. 689-697. 10.1007/s12665-009-0381-1.
38. Stetler, L., Saxton, K., (1997). Analysis of Wind Data Used for Predicting Soil Erosion. https://infosys.ars.usda.gov/WindErosion/symposium/index.htm.
39. Survey, U. (n.d.). EarthExplorer. Retrieved August 20, 2020, from https://earthexplorer.usgs.gov/.
40. Terrestrial Ecosystem Classification and Spatial Model: Mongolian Gobi Region", to this report: The Nature Conservancy. (2013). Identifying conservation priorities in the face of future development: Applying development by design in the Mongolian Gobi. The Nature Conservancy. Ulaanbaatar. . Appendix. http://www.nature.org/media/smart-development/development-by-design-gobi-english.pdf
41. Visser, S. M., Sterk, G., & Karssenberg, D. (2005). Wind erosion modelling in a Sahelian environment. Environ. Model. Softw., 20, 69-84.
42. Woodruff, N. P., & Siddoway, F. H. (1965). A Wind Erosion Equation 1. Soil Science Society of America Journal, 29(5), 602. https://doi.org/10.2136/sssaj1965.03615995002900050035x.
43. Zha, J., Wu, J., Zhao, D. et al. Future projections of the near-surface wind speed over eastern China based on CMIP5 datasets. Clim Dyn 54, 2361–2385 (2020). https://doi.org/10.1007/s00382-020-05118-4.
44. Zhang, N., Zhang, Q., Li, Y., Zeng, M., Li, W., Chan, C., Xu, Y., Huang, C., Effect of Groundcovers on Reducing Soil Erosion and Non-Point Source Pollution in Citrus Orchards on Red Soil Under Frequent Heavy Rainfall. Sustainability, 2020, 12(3):1146.
45. Zhao, H.-L., Yi, X.-Y., Zhou, R.-L., Zhao, X.-Y., Zhang, T.-H., & Drake, S. (2006). Wind erosion and sand accumulation effects on soil properties in Horqin Sandy Farmland, Inner Mongolia. CATENA, 65(1), 71–79. https://doi.org/10.1016/j.catena.2005.10.001.
46. Zhibao, D., Xunming, W., & Lianyou, L. (2000). Wind erosion in arid and semiarid China: an overview. Journal of Soil and Water Conservation, 55(4), 439-444.